Nanoscale

Accepted Manuscript

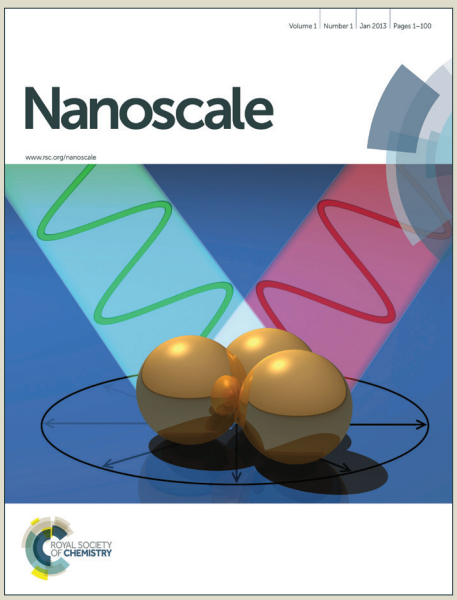

ROYAL SOCIETY OF CHEMISTRY

www.rsc.org/nanoscale

Journal Name

RSCPublishing

COMMUNICATION

Pyrite (FeS_2) Nanocrystals as Inexpensive High-Performance Lithium-Ion Cathode and Sodium-Ion Anode Materials

Marc Walter,[a,b] Tanja Zünd,[a,b] and Maksym V. Kovalenko*[a,b]

Cite this: DOI: 10.1039/x0xx00000x

Received 00th January 2012,
Accepted 00th January 2012

DOI: 10.1039/x0xx00000x

www.rsc.org/

ABSTRACT. In light of the impeding depletion of fossil fuels and necessity to lower carbon dioxide emissions, economically viable high-performance batteries are urgently needed for numerous applications ranging from electric cars to stationary large-scale electricity storage. Due to its low raw material cost, non-toxicity and potentially high charge-storage capacity pyrite (FeS_2) is a highly promising material for such next-generation batteries. In this work we present the electrochemical performance of FeS_2 nanocrystals (NCs) as lithium-ion and sodium-ion storage materials. First, we show that nanoscopic FeS_2 is a promising lithium-ion cathode material, delivering a capacity of 715 $mAhg^{-1}$ and average energy density of 1237 $Whkg^{-1}$ for 100 cycles, twice higher than for commonly used $LiCoO_2$ cathodes. Then we demonstrate, for the first time, that FeS_2 NCs can serve as highly reversible sodium-ion anode material with long cycling life. As sodium-ion anode material, FeS_2 NCs provide capacities above 500 $mAhg^{-1}$ for 400 cycles at a current rate of 1000 mAg^{-1}. In all our tests and control experiments, the performance of chemically synthesized nanoscale FeS_2 clearly surpasses bulk FeS_2 as well as large number of other nanostructured metal sulfides.

High-performance batteries are increasingly needed for numerous applications such as portable electronics, electric cars or stationary storage systems in tandem with renewable sources of electrical energy.[1, 2] Due to their high energy density lithium-ion (Li-ion) batteries (LIBs) are often considered the storage system of choice for such applications. However, in the light of limited abundance and the thereby constantly increasing costs of Li-salts, there is growing interest to develop conceptually identical sodium-ion (Na-ion) batteries (SIBs) as a potentially less expensive alternative for large-scale applications.[1, 3-5] Importantly, technology transition from LIBs to SIBs will require not only a (rather obvious) replacement of Li-ions with Na-ions, but also choosing electrode materials composed exclusively of comparably abundant elements. Herein we draw reader's attention to pyrite (FeS_2) as a promising low cost, non-toxic rechargeable electrode material for both LIBs and, for the first time, also for SIBs.

The quest for new electrode materials is primarily driven by the need to increase the energy density. The latter, in turn, is a product of charge storage capacity and voltage of operation. FeS_2 has a high theoretical specific charge-storage capacity of 894 $mAhg^{-1}$, assuming full lithiation/sodiation forming Li_2S/Na_2S+Fe. With these appealing attributes, FeS_2 is already in use as cathode material in commercial primary (non-rechargeable) Li-ion cells produced, for instance, by Energizer®. Yet the development of secondary (rechargeable) LIBs with FeS_2 has been hampered by the poor reversibility of its lithiation/delithiation at room temperature. So far, only several reports have dealt with FeS_2 as a cathode material in secondary LIBs.[6-19] For instance, Li *et al.* demonstrated FeS_2 nanooctahedra with a capacity retention of 495 $mAhg^{-1}$ after 50 cycles at 0.5C-rate (1C is current density of 894 mA g^{-1}).[15] Very little work has so far concerned mechanisms of room-temperature sodiation of FeS_2,[20-23] and high-capacity Na-ion storage, at high current densities and long-cycling life are still to be demonstrated.

In this study our aim was to enhance the reaction kinetics and reversibility of Na-ion and Li-ion storage using nanostructured FeS_2. Starting with inexpensive solution-phase chemical synthesis of nanosized FeS_2 particles, we systematically studied the performance of nano-FeS_2 as LIB and SIB electrode material and compared our results with bulk FeS_2. We find that owing to shorter diffusion path lengths for both electrons and ions, the nanoscopic counterpart exhibits highly reversible insertion of Li^+ and Na^+ ions, with near theoretical capacities. The corresponding voltage profiles indicate that nano-FeS_2 has great potential a cathode material for LIBs and as anode material for SIBs. As LIB cathode, FeS_2 NCs exhibit outstanding capacities of 720 and 600 $mAhg^{-1}$ after 50 cycles at current densities of 200 or 1000 mAg^{-1}, respectively. Further, using FeS_2 NCs for the first time as anode material in SIBs, we report high cycling stability with capacities of >500 $mAhg^{-1}$ for 400 cycles at a high current density of 1000 mAg^{-1}, making FeS_2 NCs one of the best performing SIB anodes identified so far.

The mechanism of lithiation and delithiation of FeS_2 has been established as:[14, 24]

$$FeS_2 + 2Li^+ + 2e^- \rightarrow Li_2FeS_2 \quad (1)$$

$$Li_2FeS_2 + 2Li^+ + 2e^- \rightarrow 2Li_2S + Fe \quad (2)$$

$$Fe + 2Li_2S \rightarrow Li_2FeS_2 + 2Li^+ + 2e^- \quad (3)$$

$$Li_2FeS_2 \rightarrow Li_{2-x}FeS_2 + xLi^+ + xe^- \quad (0.5<x>0.8) \quad (4)$$

$$Li_{2-x}FeS_2 \rightarrow FeS_y + (2-y)S + (2-x)Li^+ + (2-x)e^- \quad (5)$$

More specifically, the final oxidation step was proposed to yield orthorombic FeS_2 and pyrrhotite Fe_7S_8 (Equation 6).[25]

$$Li_{2-x}FeS_2 \rightarrow 0.8\text{ortho-}FeS_2 + 0.2FeS_{8/7} + 0.175S + (2\text{-}x)Li^+ + (2\text{-}x)e^- \quad (6)$$

With nanostructured active materials, not only does the reaction kinetics improve, but also the instabilities caused by the effects of large volume changes might be mitigated.[26-47] For instance, for the full sodiation of FeS_2 to Na_2S and Fe the volumetric expansion can reach 280% based on the difference in the molar volumes between the initial (FeS_2) and the final (Fe, Na_2S) phases according to $\%\Delta V = 100\% \times [2 \times V_m(Na_2S) + V_m(Fe) - V_m(FeS_2)] / V_m(FeS_2)$. Analogously, the lithiation of FeS_2 to Li_2S and Fe leads to volume changes of up to 160% or, in other words, an increase of the volume by the factor of 2.6.

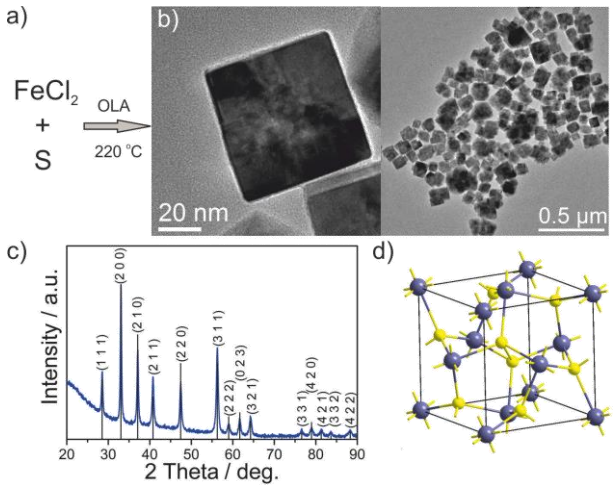

Figure 1. Synthesis and characterization of FeS_2 NCs: (a) reaction scheme; (b) transmission electron microscopy (TEM) images; (c) X-ray diffraction (XRD) pattern indexed to pure-phase pyrite FeS_2 (ICDD database, PDF No.: 00-071-2219; space group N205, *Pa3*, a = 5.4179 Å); (d) schematic representation of the unit cell of pyrite FeS_2.

We prepared FeS_2 NCs *via* adaptation of the synthesis proposed by Li *et al.*[48] In short, $FeCl_2$ and elemental S were mixed at 120 °C in oleylamine (OLA), acting as both solvent and surfactant, and reacted at 220 °C for two hours delivering highly crystalline 50-100 nm large FeS_2 NCs (Figure 1) with high reaction yield (99%). No traces of unreacted reagents, marcasite FeS_2 or other iron sulfides of different stoichiometry (FeS or Fe_3S_4) could be detected. Moreover, no traces of oxides were observed, indicating that FeS_2 NCs can be readily handled in air. Based on the low-cost, inexpensive and environmentally benign precursors, scalable heating-up reaction, and recyclable coordinating solvent (OLA), this synthesis can be readily implemented on industrial scale as well.

The electrochemical properties of the as-synthesized FeS_2 NCs were investigated in airtight coin type half-cells using either elemental lithium or sodium as both counter- and reference electrodes. The remaining surface-bound OLA molecules were removed from the NC surface by treatment with hydrazine, as commonly applied for colloidal quantum dots for improving their electronic connectivity.[49] The removal of ligands was confirmed by attenuated total reflectance Fourier transform infrared spectroscopy (ATR-FTIR) (Figure S1).

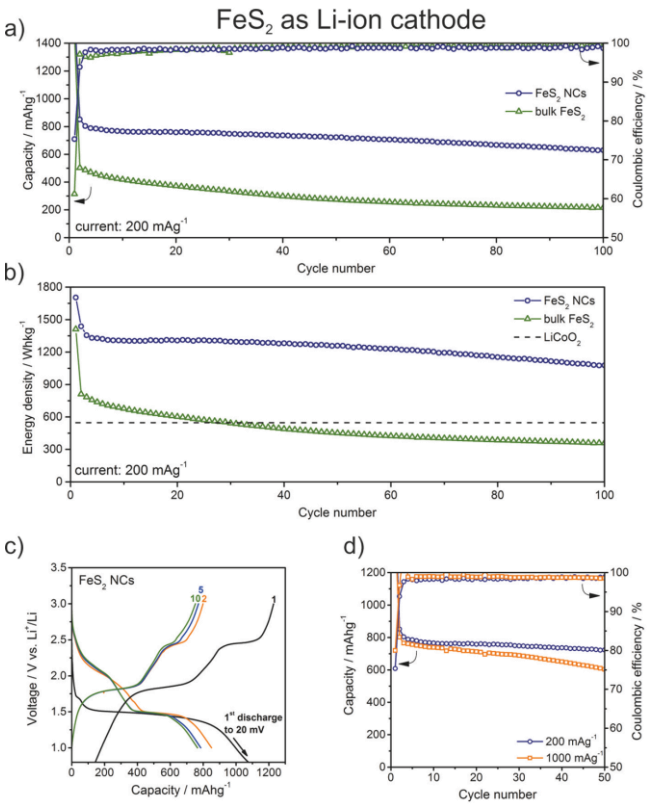

Figure 2. Electrochemical performance of FeS_2 NCs tested as cathode material for LIBs. a) Capacity retention for FeS_2 NCs and bulk FeS_2. b) Comparison of the energy density of FeS_2 NCs, bulk FeS_2 and $LiCoO_2$. c) Galvanostatic charge and discharge curves for FeS_2 NCs corresponding to the graph in a). All cells were cycled with a current rate of 200 mAg^{-1}. d) Capacity retention for FeS_2 NCs cycled at 1000 or 200 mAg^{-1}. All batteries were measured in the 1.0 – 3.0 V potential range after initial discharge to 0.02 V. 1M $LiPF_6$ in a 1:1 mixture (by weight) of ethylene carbonate (EC) and dimethylcarbonate (DMC) with 3% fluoroethylene carbonate (FEC) served as electrolyte for Li-ion half cells.

It should be noted that no changes in terms of size, shape or composition could be observed by TEM and XRD upon removal of residual OLA ligand (Figure S2) and after electrode preparation (Figures S3 and S4). All electrodes containing FeS_2 NCs were prepared by mixing the active material (64wt%) with carbon black (CB, 21%) as conductive additive and with carboxymethylcellulose (CMC, 15%) as a binder, forming a homogeneous aqueous slurry which was coated onto Cu-foil and dried. Loading of the active material was ~0.5 mg/cm^2, yielding thickness of ~15 µm. Fluoroethylene carbonate (FEC) was added to the electrolyte to improve the cycling stability.[38, 50, 51] The results for measurements of FeS_2 NCs as cathode material in Li-ion half cells are shown in Figure 2. Cells were initially discharged to 0.02 V and then cycled in the potential range between 1.0 – 3.0 V. The capacities above the theoretical value for the first cycle can be explained by the irreversible formation of the solid electrolyte interface (SEI), seen also as low coulombic efficiency (CE), that is a ratio between charge and discharge capacity), of 75% in the first cycle. Upon subsequent cycling at 200 mAg^{-1} FeS_2 NCs deliver initial capacities close to the theoretical maximum with 800 $mAhg^{-1}$ and show only minor

capacity fading during cycling (Figure 2a). Namely, after 100 cycles of charging/discharging FeS_2 NCs still deliver 630 $mAhg^{-1}$ corresponding to capacity retention of 80%. In contrast, bulk FeS_2 shows both significantly lower initial capacities and much faster fading. Despite the fact that the average lithiation potential for FeS_2 NCs is moderately low - 1.73 V (for 1.0 – 3.0 V range, Figure 2c) or 2.0 V (for 1.5 – 3.0 V range) - the high capacities result in energy densities more than twice higher than of commercially established $LiCoO_2$ or $LiFePO_4$ (Figure 2b, Table 1). Even when the current is increased to 1000 mAg^{-1}, more than 600 $mAhg^{-1}$ can be retained for 50 cycles (Figure 2d). At all current rates CE is ≥99%. To our knowledge this excellent performance in terms of obtaining high capacities at high currents is unprecedented for FeS_2 as cathode in LIBs (for detailed comparison with literature, see Table S1). It should be noted that in the absence of FEC as electrolyte additive much poorer capacity retention was observed (Figure S5).

Table 1. Comparison of Li-ion cathodic performance of FeS_2 NCs, with commercial $LiCoO_2$ and $LiFePO_4$ materials. Energy density is calculated as a product of the specific capacity and average voltage during discharge. For Li-ion full cells the lack of Li in FeS_2 might be compensated by either electrochemical prelithiation of the material or using Li-containing anode materials.[52]

Material	Capacity in $mAhg^{-1}$	Potential (vs. Li^+/Li) in V	Energy Density in $Whkg^{-1}$
FeS_2 NCs	715 (397)	1.73 (2.0)	1237 (794)
$LiCoO_2$	140	3.9	546
$LiFePO_4$	170	3.4	578

Contrary to LIBs, cycling of FeS_2 NCs as cathode material in Na-ion half cells delivers only approximately half the expected capacity and suffers from both faster capacity fading and poorer coulombic efficiency with values ranging from 98 to 96% (Figure S6). Although the performance of such FeS_2 NCs as cathode for SIBs is still superior to previous reports (for detailed comparison with literature, see Table S2),[20-23] it shows a drastic difference between Li-ion and Na-ion chemistries. Considering that in case of Na-ion cells a much higher fraction of the charge storage capacity is gained at lower potentials (Figure 3b), galvanostatic cycling measurements in the range 0.02 – 2.5 V were carried out to analyze the applicability of FeS_2 NCs as an anode material. In particular, we find that FeS_2 NCs deliver capacities of 600 $mAhg^{-1}$ after 200 cycles at a relatively high current of 1000 mAg^{-1}, and capacity of 500 $mAhg^{-1}$ after 400 cycles (Figure 3a). After 600 cycles, FeS_2 NCs still deliver capacities of 410 $mAhg^{-1}$, corresponding to 50% of the initial capacity. In contrast electrodes composed of bulk FeS_2 show much lower capacities, presumably due to slower reaction kinetics. Furthermore, for FeS_2 NCs the CE increases from approximately 97% for the first 100 cycles to an average of 99% for the subsequent cycles demonstrating good reversibility of Na-ion storage. Addition of FEC to the electrolyte was found to be crucial, since cells without FEC showed extremely poor CE of 95 – 83% (Figure 3c). Moreover, cycling tests with limitation of the charge capacity to 500 $mAhg^{-1}$ were carried out to restrict the desodiation to lower potentials, which is a preferred scenario for the full cell as it will retain largest possible potential difference between the cathode and anode and hence the energy density. No capacity fading was observed for 500 cycles at current density of 1000 mAg^{-1}. In addition, electrodes with FeS_2 NCs can be cycled with a current rate as high as 5000 mAg^{-1} and still deliver capacities above 600 $mAhg^{-1}$ for at least 50 cycles corresponding to a retention of 86% of the initial capacity (Figure 3d).

To elucidate the phase evolution during sodiation and desodation of FeS_2, *ex-situ* XRD measurements were carried out (Figure S7) at various stages of electrochemical cycling. Starting from the pristine pyrite structure of FeS_2, no intermediate crystalline phases were observed and no crystalline FeS_2 was restored during charging.

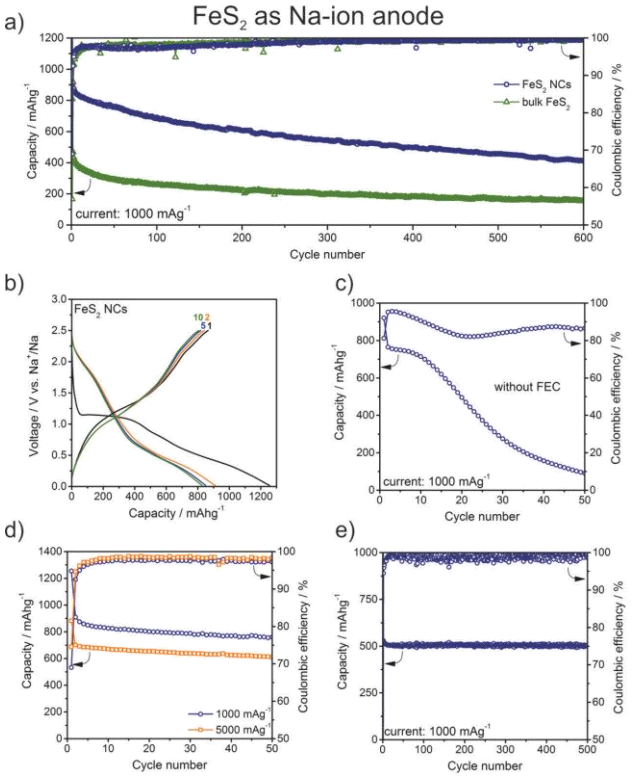

Figure 3. Electrochemical performance of FeS_2 NCs tested as anode material for SIBs. a) Capacity retention for FeS_2 NCs and bulk FeS_2. b) Galvanostatic charge and discharge curves for FeS_2 NCs corresponding to the graph in a). c) Capacity retention for FeS_2 NCs cycled with the same conditions as in a) but without the addition of FEC to the electrolyte. d) Capacity retention for FeS_2 NCs cycled with 5000 or 1000 mAg^{-1}. e) Capacity retention for FeS_2 NCs cycled with limitation of the charge capacity to 500 $mAhg^{-1}$. All batteries were measured in the 0.02 – 2.5 V potential range at a current of 1000 mAg^{-1} unless noted otherwise. 1M $NaClO_4$ in propylene carbonate (PC) with 10% fluoroethylene carbonate (FEC) served as electrolyte in Na-ion half cells.

We acknowledge the possibility that crystalline intermediate phases exist, but cannot be detected due to very small crystallite domain size in the nanometer range. Based on the observed capacities close to the theoretical value of 894 $mAhg^{-1}$ and the aforementioned reports we assume that the sodiation of FeS_2 NCs leads to the formation of Na_2S involving most likely only amorphous phases according to the following mechanism:

$$FeS_2 + 2Na^+ + 2e^- \rightarrow Na_2FeS_2 \quad (7)$$

$$Na_2FeS_2 + 2Na^+ + 2e^- \rightarrow 2Na_2S + Fe \quad (8)$$

Amorphous state during cycling may explain the apparently low kinetic restraints for fast charging/discharging and reduced

mechanical stress upon expansion and contraction, similarly to our earlier observations with Sb NCs as Na-ion anode material.[44]

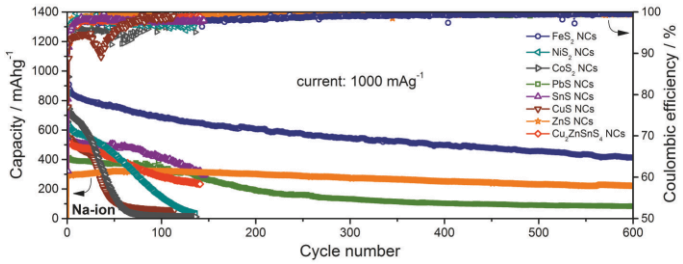

Figure 4. Electrochemical performance of various metal sulfide NCs tested as anode material for SIBs. All batteries were measured in the 0.02 – 2.5 V potential range at a constant current of 1000 mAg^{-1}. 1M $NaClO_4$ in propylene carbonate (PC) with addition of 10 wt% of fluoroethylene carbonate (FEC) served as electrolyte.

Performance of FeS_2 compares very favorably with other metal sulfides reported up to date (for detailed comparison with literature, see Table S3). For the sake of fully objective and unbiased comparison, we thus have synthesized and carefully studied, under identical testing conditions, colloidal NCs of a vast variety of prime metal sulfide candidates for Na-ion storage, composed of earth-abundant elements, such as NiS_2, CoS_2, PbS, SnS, CuS, ZnS and Cu_2ZnSnS_4 (see Figures 4 and S8). With the exception of SnS all of these sulfides had not been previously tested for Na-ion storage, judging from the available literature. Clearly, in comparison with all these sulfides, FeS_2 shows both higher initial capacity and better long-term cycling stability.

Conclusions

In conclusion, we identified and demonstrated a great potential of FeS_2 NCs as inexpensive, environmentally benign and, most importantly, high-energy-density and long-cycling electrode material for LIB cathodes and SIB anodes, outperforming bulk FeS_2 and other metal chalcogenide NCs under identical testing conditions. Cathodic Li-ion storage by FeS_2 NCs is characterized by high specific capacity of ≥630 $mAhg^{-1}$ for 100 cycles (at a current of 200 mAg^{-1}), delivering more than twice the energy density of $LiCoO_2$ or $LiFePO_4$. Anodic Na-ion storage exhibits even better overall performance, with capacities of ≥500 $mAhg^{-1}$ retained after 400 cycles at a current density of 1000 mAg^{-1}. We note that we used very standard, thus possibly suboptimal for nanostructures testing conditions in terms of selected binder, electrolytes and (most simple) electrode formulation. Future work on FeS_2 as electrode material should focus on smart electrode engineering, involving recent specific for alloying or conversion nanostructured anodes developments such as design of three-dimensional nanoarchitectures or elaborate encapsulation of nanoparticles into conductive carbons.[53-57]

Acknowledgements

This work was financially supported by ETH Zürich (Grant Nr. ETH-56 12-2), the Swiss Federal Commission for Technology and Innovation (CTI-Project Nr. 14698.2 PFIW-IW) and by CTI Swiss Competence Centers for Energy Research (SCCER Heat and Electricity Storage). We thank Loredana Protesescu for providing samples of PbS NCs. Electron microscopy was performed at Empa Electron Microscopy Center.

Notes and references

[a]ETH Zürich – Swiss Federal Institute of Technology Zürich, Vladimir Prelog Weg 1, CH-8093, Zürich, Switzerland
[b]Empa-Swiss Federal Laboratories for Materials Science and Technology, Laboratory for thin films and photovoltaics, CH-8600 Dübendorf, Switzerland
E-mail: mvkovalenko@ethz.ch

†Electronic Supplementary Information (ESI) available: materials and methods, additional structural and electrochemical characterization. See DOI: 10.1039/c000000x/

1. R. Van Noorden, *Nature*, 2014, **507**, 26-28.
2. D. Larcher and J. M. Tarascon, *Nat. Chem.*, 2015, **7**, 19-29.
3. V. Palomares, P. Serras, I. Villaluenga, K. B. Hueso, J. Carretero-Gonzalez and T. Rojo, *Energy Environ. Sci.*, 2012, **5**, 5884-5901.
4. M. D. Slater, D. Kim, E. Lee and C. S. Johnson, *Adv. Funct. Mater.*, 2013, **23**, 947-958.
5. H. Pan, Y.-S. Hu and L. Chen, *Energy Environ. Sci.*, 2013, **6**, 2338-2360.
6. E. Strauss, D. Golodnitsky and E. Peled, *Electrochem. Solid-State Lett.*, 1999, **2**, 115-117.
7. E. Strauss, D. Golodnitsky and E. Peled, *Electrochim. Acta*, 2000, **45**, 1519-1525.
8. Y. Shao-Horn, S. Osmialowski and Q. C. Horn, *J. Electrochem. Soc.*, 2002, **149**, A1547-A1555.
9. Y. Shao-Horn, S. Osmialowski and Q. C. Horn, *J. Electrochem. Soc.*, 2002, **149**, A1499-A1502.
10. E. Strauss, D. Golodnitsky, K. Freedman, A. Milner and E. Peled, *J. Power Sources*, 2003, **115**, 323-331.
11. J.-W. Choi, G. Cheruvally, H.-J. Ahn, K.-W. Kim and J.-H. Ahn, *J. Power Sources*, 2006, **163**, 158-165.
12. X. Feng, X. He, W. Pu, C. Jiang and C. Wan, *Ionics*, 2007, **13**, 375-377.
13. D. Zhang, J. P. Tu, J. Y. Xiang, Y. Q. Qiao, X. H. Xia, X. L. Wang and C. D. Gu, *Electrochim. Acta*, 2011, **56**, 9980-9985.
14. L. Li, M. Caban-Acevedo, S. N. Girard and S. Jin, *Nanoscale*, 2014, **6**, 2112-2118.
15. J. Liu, Y. Wen, Y. Wang, P. A. van Aken, J. Maier and Y. Yu, *Adv. Mater.*, 2014, **26**, 6025-6030.
16. T. Evans, D. M. Piper, S. C. Kim, S. S. Han, V. Bhat, K. H. Oh and S.-H. Lee, *Adv. Mater.*, 2014, **26**, 7386-7392.
17. T. S. Yoder, M. Tussing, J. E. Cloud and Y. Yang, *J. Power Sources*, 2015, **274**, 685-692.
18. Y. Wang, X. Qian, W. Zhou, H. Liao and S. Cheng, *RSC Advances*, 2014, **4**, 36597-36602.
19. S.-B. Son, T. A. Yersak, D. M. Piper, S. C. Kim, C. S. Kang, J. S. Cho, S.-S. Suh, Y.-U. Kim, K. H. Oh and S.-H. Lee, *Adv. Energy Mater.*, 2014, **4**, n/a-n/a.
20. T. B. Kim, J. W. Choi, H. S. Ryu, G. B. Cho, K. W. Kim, J. H. Ahn, K. K. Cho and H. J. Ahn, *J. Power Sources*, 2007, **174**, 1275-1278.
21. T. B. Kim, W. H. Jung, H. S. Ryu, K. W. Kim, J. H. Ahn, K. K. Cho, G. B. Cho, T. H. Nam, I. S. Ahn and H. J. Ahn, *J. Alloys Compd.*, 2008, **449**, 304-307.
22. A. Kitajou, J. Yamaguchi, S. Hara and S. Okada, *J. Power Sources*, 2014, **247**, 391-395.
23. Z. Shadike, Y.-N. Zhou, F. Ding, L. Sang, K.-W. Nam, X.-Q. Yang and Z.-W. Fu, *J. Power Sources*, 2014, **260**, 72-76.
24. S.-B. Son, T. A. Yersak, D. M. Piper, S. C. Kim, C. S. Kang, J. S. Cho, S.-S. Suh, Y.-U. Kim, K. H. Oh and S.-H. Lee, *Adv. Energy Mater.*, 2014, **4**, 1300961.
25. T. A. Yersak, H. A. Macpherson, S. C. Kim, V.-D. Le, C. S. Kang, S.-B. Son, Y.-H. Kim, J. E. Trevey, K. H. Oh, C. Stoldt and S.-H. Lee, *Adv. Energy Mater.*, 2013, **3**, 120-127.
26. J. B. Goodenough and Y. Kim, *Chem. Mater.*, 2009, **22**, 587-603.

27. N. Liu, Z. Lu, J. Zhao, M. T. McDowell, H.-W. Lee, W. Zhao and Y. Cui, *Nat. Nanotechnol.*, 2014, **9**, 187-192.
28. N. Nitta and G. Yushin, *Part. Part. Syst. Charact.*, 2014, **31**, 317-336.
29. C. K. Chan, H. Peng, G. Liu, K. McIlwrath, X. F. Zhang, R. A. Huggins and Y. Cui, *Nat. Nanotechnol.*, 2008, **3**, 31-35.
30. A. Magasinski, P. Dixon, B. Hertzberg, A. Kvit, J. Ayala and G. Yushin, *Nat. Mater.*, 2010, **9**, 353-358.
31. Y. Yao, M. T. McDowell, I. Ryu, H. Wu, N. Liu, L. Hu, W. D. Nix and Y. Cui, *Nano Lett.*, 2011, **11**, 2949-2954.
32. C. K. Chan, R. N. Patel, M. J. O'Connell, B. A. Korgel and Y. Cui, *ACS Nano*, 2010, **4**, 1443-1450.
33. H. Wu, G. Zheng, N. Liu, T. J. Carney, Y. Yang and Y. Cui, *Nano Lett.*, 2012, **12**, 904-909.
34. P. G. Bruce, B. Scrosati and J.-M. Tarascon, *Angew. Chem. Int. Ed.*, 2008, **47**, 2930-2946.
35. C. K. Chan, X. F. Zhang and Y. Cui, *Nano Lett.*, 2007, **8**, 307-309.
36. M.-H. Park, M. G. Kim, J. Joo, K. Kim, J. Kim, S. Ahn, Y. Cui and J. Cho, *Nano Lett.*, 2009, **9**, 3844-3847.
37. T. D. Bogart, D. Oka, X. Lu, M. Gu, C. Wang and B. A. Korgel, *ACS Nano*, 2013, **8**, 915-922.
38. A. M. Chockla, K. C. Klavetter, C. B. Mullins and B. A. Korgel, *Chem. Mater.*, 2012, **24**, 3738-3745.
39. A. M. Chockla, J. T. Harris, V. A. Akhavan, T. D. Bogart, V. C. Holmberg, C. Steinhagen, C. B. Mullins, K. J. Stevenson and B. A. Korgel, *J. Am. Chem. Soc.*, 2011, **133**, 20914-20921.
40. K. C. Klavetter, S. M. Wood, Y.-M. Lin, J. L. Snider, N. C. Davy, A. M. Chockla, D. K. Romanovicz, B. A. Korgel, J.-W. Lee, A. Heller and C. B. Mullins, *J. Power Sources*, 2013, **238**, 123-136.
41. M. R. Palacin, *Chem. Soc. Rev.*, 2009, **38**, 2565-2575.
42. S. D. Beattie, D. Larcher, M. Morcrette, B. Simon and J. M. Tarascon, *J. Electrochem. Soc.*, 2008, **155**, 158-163.
43. I. Kovalenko, B. Zdyrko, A. Magasinski, B. Hertzberg, Z. Milicev, R. Burtovyy, I. Luzinov and G. Yushin, *Science*, 2011, **333**, 75-79.
44. M. He, K. Kravchyk, M. Walter and M. V. Kovalenko, *Nano Lett.*, 2014, **14**, 1255-1262.
45. K. Kravchyk, L. Protesescu, M. I. Bodnarchuk, F. Krumeich, M. Yarema, M. Walter, C. Guntlin and M. V. Kovalenko, *J. Am. Chem. Soc.*, 2013, **135**, 4199-4202.
46. J. Qian, Y. Chen, L. Wu, Y. Cao, X. Ai and H. Yang, *Chem. Commun.*, 2012, **48**, 7070-7072.
47. L. Xiao, Y. Cao, J. Xiao, W. Wang, L. Kovarik, Z. Nie and J. Liu, *Chem. Commun.*, 2012, **48**, 3321-3323.
48. W. Li, M. Doblinger, A. Vaneski, A. L. Rogach, F. Jackel and J. Feldmann, *J. Mater. Chem.*, 2011, **21**, 17946-17952.
49. D. V. Talapin and C. B. Murray, *Science*, 2005, **310**, 86-89.
50. V. Etacheri, O. Haik, Y. Goffer, G. A. Roberts, I. C. Stefan, R. Fasching and D. Aurbach, *Langmuir*, 2011, **28**, 965-976.
51. S. Komaba, T. Ishikawa, N. Yabuuchi, W. Murata, A. Ito and Y. Ohsawa, *ACS Appl. Mater. Interfaces*, 2011, **3**, 4165-4168.
52. S. Iwamura, H. Nishihara, Y. Ono, H. Morito, H. Yamane, H. Nara, T. Osaka and T. Kyotani, *Sci. Rep.*, 2015, **5**.
53. X. Ji, K. T. Lee and L. F. Nazar, *Nat. Mater.*, 2009, **8**, 500-506.
54. X. W. Lou, C. M. Li and L. A. Archer, *Adv. Mater.*, 2009, **21**, 2536-2539.
55. H. Zhang, X. Yu and P. V. Braun, *Nat. Nanotechnol.*, 2011, **6**, 277-281.
56. Y. Yu, L. Gu, C. Wang, A. Dhanabalan, P. A. van Aken and J. Maier, *Angew. Chem. Int. Ed.*, 2009, **48**, 6485-6489.
57. N. Liu, H. Wu, M. T. McDowell, Y. Yao, C. Wang and Y. Cui, *Nano Lett.*, 2012, **12**, 3315-3321.

Table of Content Entry:

FeS_2 nanocrystals are presented as high-performance lithium-ion cathode and sodium-ion anode materials with high cycling stability